High-Resolution Rapid Prototyping of Liquid Metal Electronics by Direct Writing on Highly Prestretched Substrates

Bo Liang,[†] Jinwei Wei,[†] Lu Fang,[‡] Qingpeng Cao,[†] Tingting Tu,[†] Hangxu Ren,[†] and Xuesong Ye*,[†]

[†]College of Biomedical Engineering and Instrument Science, Zhejiang University, Hangzhou 310027, PR China
[‡]College of Life Information Science and Instrument Engineering, Hangzhou Dianzi University, Hangzhou 310018, PR China

S *Supporting Information*

ABSTRACT: A rapid and inexpensive method to produce high-resolution liquid metal patterns and electronics on stretchable substrates was introduced. Two liquid-phase gallium—indium (GaIn) alloy patterns, conductive lines, and interdigitated electrodes, were directly written or shadow mask-printed on a prestretched elastomeric substrate surface. Then, the prestretched substrate was released to recover its original length, and thus, electronic patterns simultaneously shrank on it. After these patterns were transferred to another prestretched substrate by the stamp printing method, the patterning resolution was demonstrated to increase by totally 50 times for the two successive stretch—release—shrink operations. Additionally, the resistance of the handwritten liquid metal conductive line traces remained nearly unchanged during the stretching process, which is believed to be feasible for electrical connections in stretchable electronics. The rapid prototyping of a serpentine strain sensor was successfully demonstrated to be highly sensitive and repeatable with a stretching ratio ranging from 0 to 200%. The proposed method paves a new way to fabricate stretchable electronic devices with high patterning resolution.
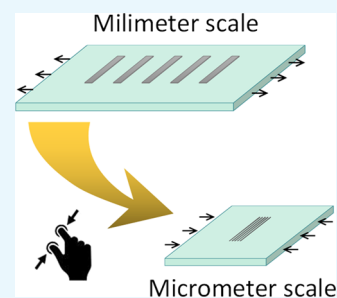
1. INTRODUCTION

Printed electronics represent an emerging area of research that could be widely commercialized because of the ability to bypass traditional expensive and rigid silicon-based electronics and fabricate electronic devices on various substrates by simple printing approaches.[1−4] Additionally, stretchable electronics take the concept of electronics one step further, where the substrate can be elongated by many times.[5−7] Stretchable electronic devices can, in principle, conform to the skin or other biological tissue or be incorporated into new form factors, such as textiles and wearable electronics.[8−10] If combined, stretchable printed electronics can thus be used in a wider application space while providing increased durability. Many printing technologies have been developed to fabricate stretchable electronic devices, such as inkjet, gravure, flexographic, and screen printing.[11] Among them, special attention has been paid to cost-effective and convenient approaches that can rapidly manufacture stretchable electronics. Recently, an alternative strategy to directly write conductive tracks on a substrate was reported.[12−16] Direct writing with various functional materials, including metal nanoparticles,[17,18] carbon nanomaterials,[19,20] and gallium-based liquid metals,[21] has been demonstrated. However, the resolution of the written conductive tracks (approximately 500 μm according to the pen) still needs further improvement.[22−24] Gallium-based liquid metals, as a new class of functional materials in printed electronics, were proposed as printing inks owing to their appealing writable properties, favorable metallic conductivity, moderate cost, and environmental friendliness.[21,25−29] Nevertheless, it remains challenging to directly write liquid metal traces with high resolution until now.[30−32]

Balloons, which are popular toys, are always preprinted with various designed figures and texts. The balloon is enlarged as air is pumped into it, resulting in the simultaneous enlargement of figures and text. This means that if we directly write or print patterns on the enlarged balloon and then deflate the balloon, the pattern resolution will be increased on the shrunk balloon. Inspired by this, we report a new method for rapid prototyping of liquid metal microscale electronic components or conductive patterns with high resolution on stretchable substrates. The liquid metal electronic patterns were first handwritten or shadow mask-printed on a prestretched elastomeric substrate surface. The high-resolution patterns were then obtained after the substrate was released. Additionally, liquid metal conductive lines, interdigitated electrodes, and serpentine strain sensors were demonstrated to be functional as stretchable electronic components by this rapid prototyping method.[33]

2. RESULTS AND DISCUSSION

The high-resolution rapid prototyping process was first achieved by direct handwriting method, as shown in Figure 1A. Liquid metal line patterns were directly written with a brush pen on a prestretched rectangular thermoplastic rubber (TPR) film, which can be stretched by 700%, as shown in Figure 1B. Then, the substrate was gently released from 700% to its original length, followed by line patterns simultaneously shrinking, and a video illustrating this is provided in the
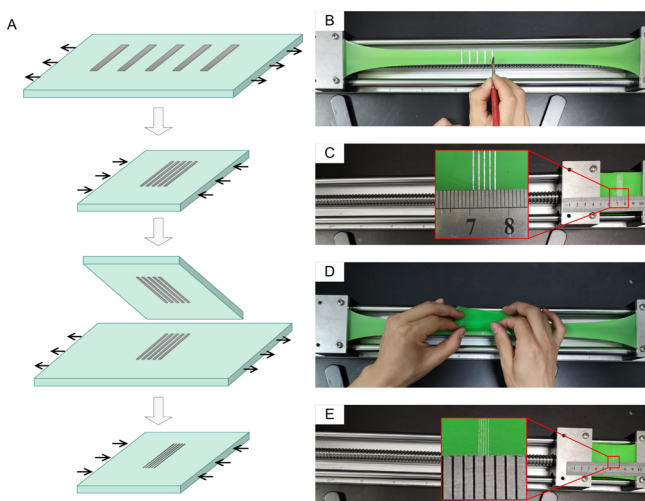
Figure 1. (A) Schematic and (B−E) photographs of the fabrication process of high-resolution liquid metal patterns by (B) handwriting line traces on a prestretched substrate, (C) releasing the stretched substrate, (D) transfer printing the line traces to another prestretched substrate, and (E) releasing the second stretched substrate.

Supporting Information, Movie S1. The gap between the line patterns decreased from 10 mm (Figure 1B) to ∼1.5 mm (Figure 1C), and the line width exhibited similar narrowing behavior. Thus, the patterning resolution was increased by nearly seven times in this step.

The shrunk patterns from Figure 1C were transferred onto another prestretched TPR substrate by using the stamp printing method, where the top patterned film became the "soft" stamp.[34−36] The "soft" stamp was gently pressed on the bottom TPR substrate and withdrawn carefully, leaving the patterns on it. The TPR substrate was chosen here because it exhibited better wettability and adhesion to the gallium-based liquid metals, which is enough to maintain the shapes and structures of patterns. Thus, liquid metal patterns can be easily printed and transferred onto the TPR substrates without intolerable agglomerations, which could cause pattern damages on other substrates. Note that too much pressure in this manual transfer would cause one line pattern merge with another, resulting in a failed transfer. Because the gap of them became narrower, the line patterns were more likely to merge by manual operations, and thus, the transfer process failed more easily. After that, the bottom TPR substrate was released to further improve the resolution of the transferred patterns (Supporting Information, Movie S2), as shown in Figure 1D,E. Generally, the patterning resolution in the above two successive stretch−release−shrink processes is boosted by nearly 50 times. To evaluate the minimum line width that can be achieved from this approach, we wrote liquid metal lines with initial width of 500 μm (Figure 2A) on a 500%

prestretched substrate. After releasing the substrate, the line width decreased to 100 μm (Figure 2B). Followed with the transfer printing and releasing process on another 500% prestretched substrate, the final line width of the liquid metal lines was about 20−25 μm (Figure 2C). It should be noted that the highest resolution by the proposed approach was limited by the manual operation; thus, it can be further improved through machine assistance. This approach for printing high-resolution liquid metal traces also makes handwriting an effective method for rapid prototyping of high-quality liquid metal stretchable electronics.

In comparison to handwriting, the shadow mask printing techniques feature delicate pattern designs, mass production, and device consistency when employed in rapid prototyping of electronic devices. Therefore, the shadow mask printing method was demonstrated to be feasible for producing high-resolution liquid metal patterns on TPR substrates. A schematic of printing high-resolution liquid metal patterns on a prestretched substrate with a shadow mask is illustrated in Figure 3A. As shown in Figure 3B,C, the electrode gap in the well-designed interdigitated electrode pattern narrowed down to one-seventh of the original gap after the stretchable substrate was released. Additionally, the serpentine line pattern exhibited the same scaling behaviors in Figure 3D,E, before and after the release of the stretched substrate, respectively. The serpentine line width narrowed from 200 to 50 μm in the TPR release process, as shown in the optical microscopic images of Figure 3F,G.

After the liquid metal ink was written on the substrate, a gallium oxide skin formed on the surface of line traces, allowing the written pattern to maintain its shape. Because the liquid metal traces have both low fluidic viscosity and high surface tension, the printed pattern can simultaneously behave like a solid and a liquid. The suitability of handwritten liquid metal line patterns was further demonstrated for conductive lines used in stretchable electronics, in which the resistance of the conductive lines should remain nearly unchanged when the substrate was stretched. In Figure 4A, eight parallel line traces handwritten on a 700% stretched substrate, with the original line width ranging from 1.6 to 2.8 mm, were chosen to show morphological evolution after the substrate was released step-by-step from 700 to 100%. The line width generally decreased linearly from the original width to ∼300 μm, with the stretching ratio of the substrate becoming smaller in Figure 4B. Fortunately, the resistance of all eight written traces as a function of the substrate stretching ratio remained nearly unchanged during the whole process, as shown in Figure 4C. All of these features make liquid metal line patterns practical for stretchable electronic applications.

In addition, a strain sensor was successfully fabricated by handwriting the serpentine line patterns on the stretchable substrate as a simple demonstration of the liquid metal
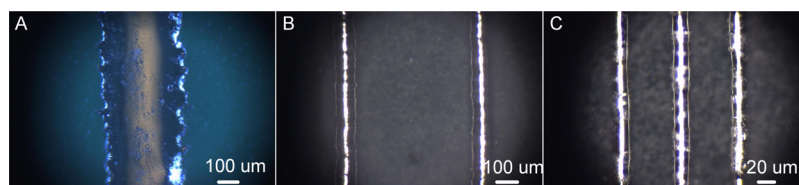

Figure 2. Microscopic images of liquid metal line pattern microstructures before the prestretched substrate releasing (A), after the substrate releasing (B), and after the transfer printing and releasing process (C).
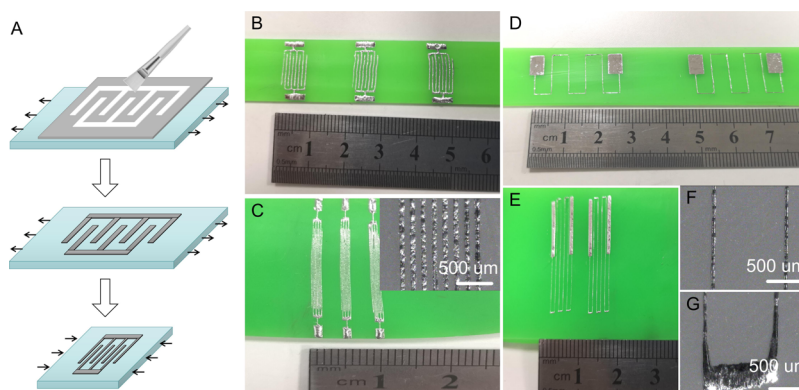
Figure 3. (A) Schematic of printing high-resolution liquid metal patterns on a prestretched substrate with a shadow mask and then releasing the stretched substrate. Photographs of the printed interdigitated electrode patterns (B) before and (C) after the release of the stretched substrate. Photographs of the printed serpentine line patterns (D) before and (E) after release of the stretched substrate. (F,G) Optical microscopic images of the printed serpentine line patterns.
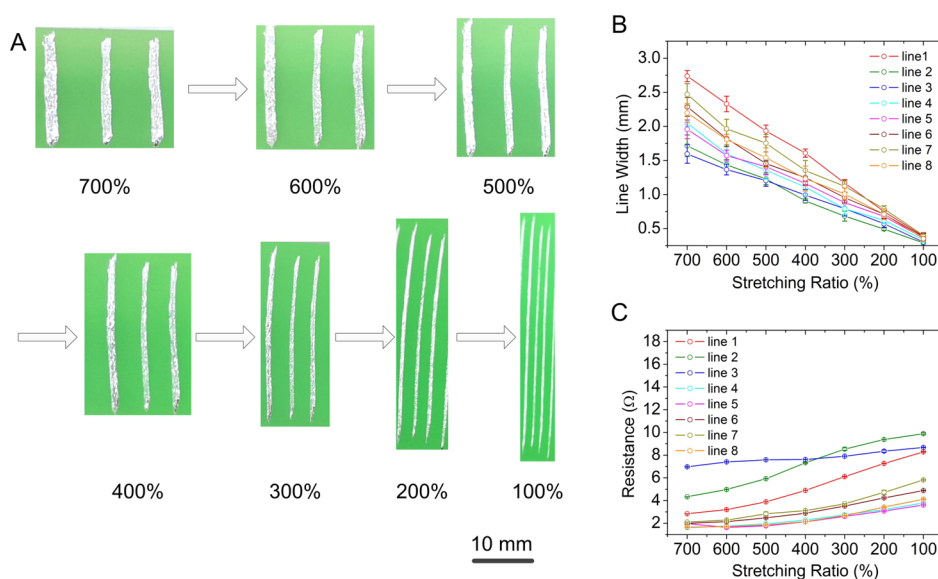

Figure 4. (A) Morphology evolution of handwritten line traces upon releasing the prestretched substrate. (B) Line width of the handwritten traces as a function of the substrate stretching ratio. (C) Line resistance of the handwritten traces as a function of the substrate stretching ratio.

electronic device. It was also prestretched by a ratio of 700% and released. The stress−strain tests were conducted in the horizontal (Figure 5B) and vertical (Figure 5D) directions. Figure 5A shows that the normalized resistance of the serpentine strain sensor, stretched in the horizontal direction, gradually decreased as the applied strain increased and then increased after the strain exceeded 400%. In Figure 5B, the normalized resistance of the sensor exhibited a monotonous response behavior as the applied strain increased from 0 to 200% in the vertical direction.

According to the different sensing behaviors, the sensing mechanism of the strain sensor in different directions was briefly illustrated as follows: it was known that the resistance R of line conductive traces can be obtained by

$$R = \rho \times \frac{L}{S}$$

where ρ is the resistivity of liquid metal, L is the line length, and S is the cross-section area. Because each serpentine sensor can be divided into long line segments perpendicular to the stretching direction and short ones parallel to the stretching direction, the whole resistance R can be presented by

$$R = R_l + R_s = \rho \times \frac{L_l}{S_l} + \rho \times \frac{L_s}{S_s}$$

where L_l and L_s are line lengths of long segments and short ones, respectively, and S_l and S_s are cross-section areas of long segments and short ones.

When horizontally stretched, the length of long segments L_l decreased and their cross-section area S_l increased simultaneously. It was attributed to the fact that volume V of the line pattern is constant during stretching, which is the product of the cross-section area and line length. Thus, the resistance of long line segments R_l decreased. In contrast, the length L_s exhibited an increasing trend and cross-section area S_s of the short segments a decreasing trend, resulting in the whole increased resistance of short line segments. When the stretching ratio is below 400%, the whole normalized resistance changes of the sensor mainly came from that of the long segments in the horizontal stretching direction, while the short line changes had little impact. Correspondingly, the whole
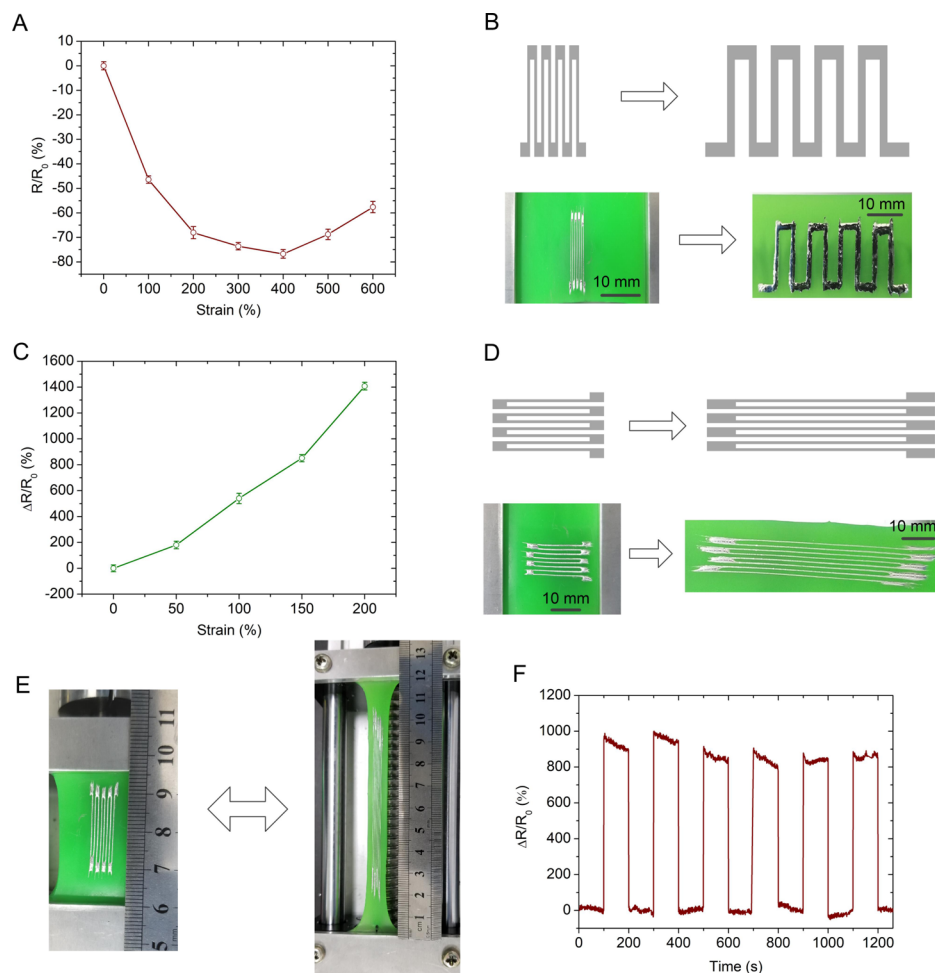
Figure 5. (A) Normalized resistance changes (defined as $\Delta R/R_0$, $\Delta R = R - R_0$) with substrate stretching in the horizontal direction. (B) Schematics and photographs of the horizontal stretching test. (C) Normalized resistance changes with substrate stretching in the vertical direction. (D) Schematics and photographs of the vertical stretching test. (E) Photographs of dynamic tests stretching in the vertical direction. (F) Dynamic responses of 150% strain repeating tests in the vertical direction.

resistance gradually decreased. When stretching beyond the critical level, the changes of short segments started to take a dominant role, although the long segments may still exhibit unnoticeable changes. It should be noted that the parabolic sensing performance and low sensitivity made this structure unsuitable as a strain sensor which was stretched horizontally.

In the vertical stretching case, the long segments always made a significant contribution to the normalized resistance changes. When vertically stretched, the length of the long line segments extended and their cross-section area decreased simultaneously, resulting in a monotonous response behavior and high sensitivity. Additionally, the dynamic responses under an applied strain of 150% were recorded in Figure 5E,F to evaluate its repeatability as a strain sensor. It was highly repeatable within a strain range of 150%.

3. CONCLUSIONS

In summary, high-resolution liquid-phase gallium−indium (GaIn) alloy patterns, such as conductive lines or interdigitated electrodes, were successfully obtained. The designed patterns were achieved by handwriting or shadow mask printing on a prestretched elastomeric substrate surface and then releasing the substrate. With the help of the transfer printing method, the liquid metal pattern resolution was improved by nearly 50

times after two successive stretch−release−shrink processes of the substrate. Additionally, the resistance of the written line patterns was demonstrated to remain almost unchanged regardless of how much the substrate was stretched. This demonstrated that written line patterns are suitable candidates for conductive lines in stretchable electronics. In addition, a highly sensitive and repeatable strain sensor was fabricated as a proof-of-concept when used in the vertical stretching direction. The progress made here may pave a new way to design and build high-resolution liquid metal electronic patterns or devices in stretchable electronics.

4. EXPERIMENTAL SECTION

4.1. Materials. *4.1.1. Liquid metal ink.* Gallium and indium metals with a weight ratio of 90:10, according to the chemical composition of GaIn10 alloy, were purchased from Shenyang Northeast Nonferrous Metal Market Co., Ltd. (Shenyang, China) and used as the conductive ink. The GaIn10 liquid metal ink was stirred for 10 min with a stir speed of 200 rpm to obtain a composite of GaIn10 alloy and a small amount of uniformly dispersed gallium oxide with appropriate viscosity.

4.1.2. Stretchable substrate. TPR elastomer was purchased from Walmart Supermarket and chosen as the substrate

material due to its highly stretchable property. Rectangular TPR films cut from a TPR inflatable jelly balloon ball were directly used for direct writing after scrubbing with ethyl alcohol.

4.1.3. Equipment. The stretching machine was constructed in the laboratory by combining a sliding rail (model: 1024, purchased from Taizhou Hengchuang Transmission Technology Co., Ltd.) with a stepping motor (model: 86BYG250H, purchased from Shenzhen Yixing Electronic Co., Ltd.) with a maximum output torque of 12 N m. The resistance of the liquid metal patterns was measured using an Agilent 34401A Digital Multimeter. The automatic continuous measurement and data recording was implemented by executing the Python script written in the Spyder platform.

4.2. Direct Writing Process. Line patterns were directly written on the TPR films with a brush pen for simple functional demonstration, in which the TPR film was first stretched up to 700%. The original line width was 2 ± 0.5 mm with a line gap of approximately 10 mm. Afterward, the stretched film with written patterns was released, and thus, the pattern shrank to one-seventh of its original size with a line width of 275 ± 75 μm and a line gap of less than 1.5 mm.

Then, we transfer printed the line pattern to another TPR film stretched up to 700%. When the stretched film was released, the pattern shrank to a further decreased size. The optical microscopic image showed that the line width was reduced to approximately 37.5 ± 12.5 μm and the line gap was reduced to 200 μm. Thus, the printing resolution was increased by nearly 50 times through the above two simple steps. The final line width would be wider than the theoretical calculated value because the line traces were widened during the transfer printing operation. Generally, the pattern size could be reduced further by repeating the transfer step. However, overlap of line traces would occur during manual transfer printing because of the narrow line gaps.

Complex patterns, like interdigitated electrodes and serpentine lines, could also be directly written by using a brush pen. Additionally, the transfer printing method could be used to improve the resolution of complex patterns, just like with the line pattern writing process.

4.3. Shadow Mask Printing Process. The patterns on the shadow mask were designed in CorelDRAW Graphical Suite X7. The line width of the interdigitated electrode pattern was set to 200 μm, and the gap distance was 1 mm. The line width of the serpentine line pattern was 200 μm, and the gap was 5 mm. Then, the shadow mask was fabricated by laser cutting the stainless steel sheet with a thickness of 100 μm. The obtained shadow mask, the painting pen, and the substrate were rinsed in ethanol for thorough cleaning before the printing process. After that, the shadow mask was placed onto the substrate before the liquid metal was brushed on it by the painting pen. Therefore, the liquid metal could penetrate the patterns on the mask and reach the substrate surface.

■ ASSOCIATED CONTENT

ⓢ Supporting Information
The Supporting Information is available free of charge at https://pubs.acs.org/doi/10.1021/acsomega.9b02440.

> Release of the prestretched substrate with hand written line patterns (AVI)
>
> Release of the prestretched substrate with transfer printed patterns (AVI)

■ AUTHOR INFORMATION

Corresponding Author
*E-mail: yexuesong@zju.edu.cn.
ORCID ⓘ
Qingpeng Cao: 0000-0002-1492-4680
Xuesong Ye: 0000-0002-3439-3733
Author Contributions
These authors contributed equally. The manuscript was written through contributions of all authors. All authors have given approval to the final version of the manuscript.
Notes
The authors declare no competing financial interest.

■ REFERENCES

(1) Perelaer, J.; Smith, P. J.; Mager, D.; Soltman, D.; Volkman, S. K.; Subramanian, V.; Korvink, J. G.; Schubert, U. S. Printed Electronics: The Challenges Involved in Printing Devices, Interconnects, and Contacts Based on Inorganic Materials. *J. Mater. Chem.* **2010**, *20*, 8446−8453.

(2) Bandodkar, A. J.; Nuñez-Flores, R.; Jia, W.; Wang, J. All-Printed Stretchable Electrochemical Devices. *Adv. Mater.* **2015**, *27*, 3060−3065.

(3) Li, D.; Lai, W.-Y.; Zhang, Y.-Z.; Huang, W. Printable Transparent Conductive Films for Flexible Electronics. *Adv. Mater.* **2018**, *30*, 1704738.

(4) Lewis, J. A.; Ahn, B. Y. Device Fabrication: Three-Dimensional Printed Electronics. *Nature* **2015**, *518*, 42.

(5) Rogers, J. A.; Someya, T.; Huang, Y. Materials and Mechanics for Stretchable Electronics. *science* **2010**, *327*, 1603−1607.

(6) Wagner, S.; Bauer, S. Materials for Stretchable Electronics. *MRS Bull.* **2012**, *37*, 207−213.

(7) Cheng, T.; Zhang, Y.; Lai, W.-Y.; Huang, W. Stretchable Thin-Film Electrodes for Flexible Electronics with High Deformability and Stretchability. *Adv. Mater.* **2015**, *27*, 3349−3376.

(8) Bandodkar, A. J.; You, J.-M.; Kim, N.-H.; Gu, Y.; Kumar, R.; Mohan, A. M. V.; Kurniawan, J.; Imani, S.; Nakagawa, T.; Parish, B.; Parthasarathy, M.; Mercier, P. P.; Xu, S.; Wang, J. Soft, Stretchable, High Power Density Electronic Skin-Based Biofuel Cells for Scavenging Energy from Human Sweat. *Energy Environ. Sci.* **2017**, *10*, 1581−1589.

(9) Wang, S.; Xu, J.; Wang, W.; Wang, G.-J. N.; Rastak, R.; Molina-Lopez, F.; Chung, J. W.; Niu, S.; Feig, V. R.; Lopez, J.; Lei, T.; Kwon, S.-K.; Kim, Y.; Foudeh, A. M.; Ehrlich, A.; Gasperini, A.; Yun, Y.; Murmann, B.; Tok, J. B.-H.; Bao, Z. Skin Electronics from Scalable Fabrication of an Intrinsically Stretchable Transistor Array. *Nature* **2018**, *555*, 83.

(10) Lee, Y.; Kim, J.; Jang, B.; Kim, S.; Sharma, B. K.; Kim, J.-H.; Ahn, J.-H. Graphene-Based Stretchable/Wearable Self-Powered Touch Sensor. *Nano Energy* **2019**, *62*, 259−267.

(11) Khan, S.; Ali, S.; Bermak, A. Recent Developments in Printing Flexible and Wearable Sensing Electronics for Healthcare Applications. *Sensors* **2019**, *19*, 1230.

(12) Tai, Y.-L.; Yang, Z.-G. Fabrication of Paper-Based Conductive Patterns for Flexible Electronics by Direct-Writing. *J. Mater. Chem.* **2011**, *21*, 5938−5943.

(13) Kurra, N.; Kulkarni, G. U. Pencil-on-Paper: Electronic Devices. *Lab Chip* **2013**, *13*, 2866−2873.

(14) Jia, H.; Wang, J.; Zhang, X.; Wang, Y. Pen-Writing Polypyrrole Arrays on Paper for Versatile Cheap Sensors. *ACS Macro Lett.* **2013**, *3*, 86−90.

(15) Han, Y. L.; Hu, J.; Genin, G. M.; Lu, T. J.; Xu, F. Biopen: Direct Writing of Functional Materials at the Point of Care. *Sci. Rep.* **2015**, *4*, 4872.

(16) Grey, P.; Gaspar, D.; Cunha, I.; Barras, R.; Carvalho, J. T.; Ribas, J. R.; Fortunato, E.; Martins, R.; Pereira, L. Handwritten Oxide Electronics on Paper. *Adv. Mater. Technol.* **2017**, *2*, 1700009.

(17) Huang, Y.; Zhang, W.; Wang, J.; Wei, Z. Probing the Sensory Property of Perylenediimide Derivatives in Hydrazine Gas: Core-Substituted Aromatic Group Effect. *ACS Appl. Mater. Interfaces* **2014**, *6*, 9307−9313.

(18) Wang, R.; Liu, Y.; Bai, B.; Guo, N.; Guo, J.; Wang, X.; Liu, M.; Zhang, G.; Zhang, B.; Xue, C.; Liu, J.; Zhang, W. Wide-Frequency-Bandwidth Whisker-Inspired Mems Vector Hydrophone Encapsulated with Parylene. *J. Phys. D: Appl. Phys.* **2016**, *49*, 07LT02.

(19) Cheng, C.; Zhang, J. G.; Li, S.; Xia, Y.; Nie, C. X.; Shi, Z. Q.; Cuellar-Camacho, J. L.; Ma, N.; Haag, R. A Water-Processable and Bioactive Multivalent Graphene Nanoink for Highly Flexible Bioelectronic Films and Nanofibers. *Adv. Mater.* **2018**, *30*, 1870303.

(20) Yang, W.; Wang, C. Graphene and the Related Conductive Inks for Flexible Electronics. *J. Mater. Chem. C* **2016**, *4*, 7193−7207.

(21) Dickey, M. D. Stretchable and Soft Electronics Using Liquid Metals. *Adv. Mater.* **2017**, *29*, 1606425.

(22) Russo, A.; Ahn, B. Y.; Adams, J. J.; Duoss, E. B.; Bernhard, J. T.; Lewis, J. A. Pen-on-Paper Flexible Electronics. *Adv. Mater.* **2011**, *23*, 3426−3430.

(23) Lin, Y.; Cooper, C.; Wang, M.; Adams, J. J.; Genzer, J.; Dickey, M. D. Handwritten, Soft Circuit Boards and Antennas Using Liquid Metal Nanoparticles. *Small* **2015**, *11*, 6397−6403.

(24) Quain, E.; Mathis, T. S.; Kurra, N.; Maleski, K.; Van Aken, K. L.; Alhabeb, M.; Alshareef, H. N.; Gogotsi, Y. Direct Writing of Additive-Free Mxene-in-Water Ink for Electronics and Energy Storage. *Adv. Mater. Technol.* **2019**, *4*, 1800256.

(25) Mohammed, M. G.; Kramer, R. All-Printed Flexible and Stretchable Electronics. *Adv. Mater.* **2017**, *29*, 1604965.

(26) Boley, J. W.; White, E. L.; Chiu, G. T.-C.; Kramer, R. K. Direct Writing of Gallium-Indium Alloy for Stretchable Electronics. *Adv. Funct. Mater.* **2014**, *24*, 3501−3507.

(27) Ladd, C.; So, J.-H.; Muth, J.; Dickey, M. D. 3d Printing of Free Standing Liquid Metal Microstructures. *Adv. Mater.* **2013**, *25*, 5081−5085.

(28) Wang, Q.; Yu, Y.; Yang, J.; Liu, J. Fast Fabrication of Flexible Functional Circuits Based on Liquid Metal Dual-Trans Printing. *Adv. Mater.* **2015**, *27*, 7109−7116.

(29) Tavakoli, M.; Malakooti, M. H.; Paisana, H.; Ohm, Y.; Green Marques, D.; Alhais Lopes, P.; Piedade, A. P.; de Almeida, A. T.; Majidi, C. Egain-Assisted Room-Temperature Sintering of Silver Nanoparticles for Stretchable, Inkjet-Printed, Thin-Film Electronics. *Adv. Mater.* **2018**, *30*, 1801852.

(30) Zhang, S.; Wang, B.; Jiang, J.; Wu, K.; Guo, C. F.; Wu, Z. High-Fidelity Conformal Printing of 3d Liquid Alloy Circuits for Soft Electronics. *ACS Appl. Mater. Interfaces* **2019**, *11*, 7148−7156.

(31) Liu, J.; Yang, S.; Liu, Z.; Guo, H.; Liu, Z.; Xu, Z.; Liu, C.; Wang, L. Patterning Sub-30 μm Liquid Metal Wires on Pdms Substrates Via Stencil Lithography and Pre-Stretching. *J. Micromech. Microeng.* **2019**, *29*, 095001.

(32) Kim, D.; Yoon, Y.; Kauh, S. K.; Lee, J. Towards Sub-Microscale Liquid Metal Patterns: Cascade Phase Change Mediated Pick-N-Place Transfer of Liquid Metals Printed and Stretched over a Flexible Substrate. *Adv. Funct. Mater.* **2018**, *28*, 1800380.

(33) Sahlberg, A.; Nilsson, F.; Berglund, A.; Nguyen, H.; Hjort, K.; Jeong, S. H. High-Resolution Liquid Alloy Patterning for Small Stretchable Strain Sensor Arrays. *Adv. Mater. Technol.* **2018**, *3*, 1700330.

(34) Sharp, K. G.; Blackman, G. S.; Glassmaker, N. J.; Jagota, A.; Hui, C.-Y. Effect of Stamp Deformation on the Quality of Microcontact Printing: Theory and Experiment. *Langmuir* **2004**, *20*, 6430−6438.

(35) Xia, Y.; Whitesides, G. M. Reduction in the Size of Features of Patterned Sams Generated by Microcontact Printing with Mechanical Compression of the Stamp. *Adv. Mater.* **1995**, *7*, 471−473.

(36) Meitl, M. A.; Zhu, Z.-T.; Kumar, V.; Lee, K. J.; Feng, X.; Huang, Y. Y.; Adesida, I.; Nuzzo, R. G.; Rogers, J. A. Transfer Printing by Kinetic Control of Adhesion to an Elastomeric Stamp. *Nat. Mater.* **2006**, *5*, 33−38.